THE JOURNAL OF PHYSICAL CHEMISTRY B

Article

pubs.acs.org/JPCB

Direct Observation of Ligand Rebinding Pathways in Hemoglobin Using Femtosecond Mid-IR Spectroscopy

Seongheun Kim, Jaeheung Park, Taegon Lee, and Manho Lim*

Department of Chemistry and Chemistry Institute for Functional Materials, Pusan National University, Busan 609-735, Korea

Supporting Information

ABSTRACT: The dynamics of NO rebinding in hemoglobin (Hb) was directly observed using femtosecond mid-IR spectroscopy after photodeligation of NO from HbNO in D_2O at 283 K. Time-resolved spectra of bound NO appeared to have a single feature peaked at 1616 cm^{-1} but were much better described by two Gaussians with equal intensities but different rebinding kinetics, where the feature at 1617 cm^{-1} rebinds faster than the one at 1614 cm^{-1}. It is possible that the two bands each correspond to one of two subunit constituents of the tetrameric Hb. Transient absorption spectra of photodeligated NO revealed three evolving bands near 1858 cm^{-1} and their red-shifted replicas. The red-shifted replicas arise from photodeligated NO in the vibrationally excited $v = 1$ state. More than 10% of the NO was dissociated into the vibrationally excited $v = 1$ state when photolyzed by a 580 nm pulse. The three absorption bands for the deligated NO could be attributed to three NO sites in or near the heme pocket. The kinetics of the three transient bands for the deligated NO, as well as the recovery of the bound NO population, was most consistent with a kinetics scheme that incorporates time-dependent rebinding from one site that rapidly equilibrates with the other two sites. The time dependence results from a time-dependent rebinding barrier due to conformational relaxation of protein after deligation. By assigning each absorption band to a site in the heme pocket of Hb, a pathway for rebinding of NO to Hb was proposed.

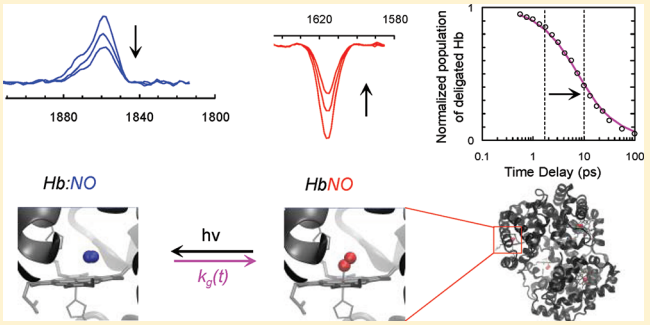

I. INTRODUCTION

The dynamics of ligand binding to heme proteins such as myoglobin (Mb) and hemoglobin (Hb) has been widely studied as a model system for investigating the relationships between protein dynamics, structure, and function.[1] In particular, the most extensively investigated phenomena, both theoretically and experimentally, have been the rebinding of CO following photodeligation of MbCO under various conditions.[1,2] Under physiological conditions, most of the CO deligated from MbCO tends to escape to solution without geminate rebinding (GR),[3] and thus MbCO is more useful for studying the conformational relaxation of the heme protein after photodeligation than GR. In contrast, the NO deligated from MbNO or HbNO rebinds very efficiently on the picosecond (ps) time scale.[4−7] Therefore, the rebinding of NO to these heme proteins has been used to examine how protein dynamics control the binding of the ligand (the protein's function) under physiological conditions.[7,8]

The kinetics of rebinding of NO to a heme protein has mainly been probed using time-resolved visible spectroscopy, which is sensitive to electronic transitions of the heme chromophore. Time-resolved visible absorption spectra were used to extract the time dependence of the populations of NO-bound protein and deligated protein after photodeligation of the NO-ligated protein. These investigations showed the kinetics of GR of NO to the heme protein.[4−6,9−17] However, visible absorption spectroscopy cannot probe the deligated NO directly and therefore can provide very little, if any, information regarding the whereabouts of the deligated ligand or the rebinding pathway. The deligated NO can be readily detected by probing the stretching mode of NO. Since the vibrational spectrum of a molecule is very sensitive to its environment, mid-IR spectroscopy of NO can be an excellent probe of the NO's location after deligation. Furthermore, since the bound ligand has multiple vibrational bands that are attributed to different protein structures (conformational substates, CSs)[18] of ligand-bound protein such as MbCO and MbNO, time-resolved vibrational spectroscopy can measure conformer-dependent rebinding kinetics. Different rebinding kinetics was measured for each CO band in low-temperature MbCO,[19] and this result was used to suggest that at low temperatures MbCO has conformer-dependent rebinding rates. For MbNO at room temperature, different NO bands had the same rebinding kinetics, indicating that it has conformer-independent rebinding rates.[7] Multiple vibrational bands were also observed for the deligated ligand and have been attributed to different positions and/or orientations of the deligated ligand within the protein near the Fe atom in a given CS.[18,20] Therefore, femtosecond

Received: March 20, 2012
Revised: May 11, 2012
Published: May 15, 2012

(fs) vibrational spectroscopy may show the NO's location and its pathway to rebinding by directly probing the NO deligated from NO-bound heme proteins as well as conformer-dependent rebinding rates.

Recently, we investigated the dynamics of the rebinding of NO to Mb after photodeligation of MbNO in D_2O at 283 K using fs mid-IR spectroscopy and showed that MbNO has conformer-independent rebinding rates.[7] We also observed three bands of the NO deligated from MbNO (denoted as B state) and attributed them to NO in three different sites within or near the heme pocket. A kinetics scheme was extracted from both the kinetics of the deligated NOs in three sites and the recovery kinetics of the MbNO population.[8] This kinetics scheme, which incorporates rebinding from a B state with a time-dependent barrier and interconversion among three B states, was used to envision a pathway for the rebinding of NO to Mb.[8] Here, we extend our previous work on MbNO to a tetrameric heme protein, Hb.

The dynamics of GR of NO to Hb in D_2O at 283 K was measured by simultaneously probing the recovery kinetics of the ligand's bound form and the transient kinetics of new absorption bands arising from NO in or near the heme pocket. The recovery kinetics is nonexponential, and more than 90% of the NO rebinds within 100 ps. Three B bands were observed, and their transient behaviors were found to be very similar to those observed in MbNO, although there was a faster rate for HbNO. From the observed kinetics of bound and deligated NO, a pathway for rebinding of NO to HbNO was proposed.

II. EXPERIMENTAL DETAILS

A 2−2.4 mM HbNO (8−9.6 mM heme) sample was prepared by dissolving lyophilized human hemoglobin A (Sigma) in deoxygenated D_2O buffered with 0.1 M potassium phosphate (pD = 7.4). It was reduced with a 2-fold excess of freshly prepared sodium dithionate (Aldrich), and an equivalent quantity of 0.1 M degassed sodium nitrite (Aldrich) solution was added in the presence of an equimolar quantity of 0.1 M sodium dithionate.[21] All sample preparations were carried out in an ice bath to minimize thermal denaturation. To remove light-scattering sources such as dust particles and denatured protein aggregates, the samples were filtered through a 5 μm membrane filter before being loaded in a gastight flowing[22] or rotating sample cell with two 2 mm thick CaF_2 windows. Use of a rotating sample cell results in higher noise due to inhomogeneous scattering from the cell window, and the flowing cell requires a path length of >50 μm for flowing the concentrated protein sample. Whereas a flowing cell with a path length of 100 μm was used for collecting spectra of NO photodeligated from HbNO, a rotating cell with a path length of 9 μm was used to collect spectra of the NO band in HbNO to minimize the influence of the strong background absorption near 1610 cm^{-1} arising from the amide I band and water. Throughout the experiments, the integrity and concentration of the sample were routinely checked using UV−vis and FT-IR spectroscopy. During data collection, the sample cell was either flowed or rotated sufficiently fast so that each photolyzing laser pulse illuminated a fresh volume of the sample. The sample was prepared in D_2O to isotopically shift the spectral region of interest to a region with greater IR transmission. The temperature of the sample cell was kept at 283 ± 1 K.

The details of the time-resolved mid-IR spectrometer used here are described elsewhere.[7] Briefly, two identical home-built optical parametric amplifiers (OPA) pumped by a commercial Ti:sapphire amplifier with a repetition rate of 1 kHz are used to generate a visible pump pulse and a mid-IR probe pulse. The signal pulse of one OPA is frequency doubled in a type I, 1 mm thick BBO crystal to generate a tunable pump pulse in the visible region. The signal and idler pulse of the other OPA are difference-frequency mixed in a 1 mm thick, type I $AgGaS_2$ crystal to yield a tunable mid-IR pulse (110 fs, 160 cm^{-1}, 1 μJ). A small portion of this pulse is used to probe the transient mid-IR absorbance of the sample photolyzed by 3 μJ, 580 nm pulses. The polarization of the pump pulse was set at the magic angle (54.7°) relative to the probe pulse to recover the isotropic absorption spectrum. The broadband transmitted probe pulse is detected with a 64-element N_2(l)-cooled HgCdTe array detector. The array detector is mounted in the focal plane of a 320 mm monochromator with a 150 lines/mm grating, resulting in a spectral resolution of ca. 1.4 cm^{-1}/pixel at 1800 cm^{-1}. Because of the excellent short-term stability of the IR light source (<0.5% rms), the pump-induced change in the absorbance of the sample ΔA is routinely computed to a precision of $<1 \times 10^{-4}$ rms after 0.5 s of signal averaging. The pump spot was made to be about 1.5 times larger than the probe spot (ca. 120 μm diameter) to ensure spatially uniform photoexcitation across the spatial dimensions of the probe pulse. Moderate pump energy and an enlarged photolysis beam size also minimize the spatial thermal effects. The instrument response function, determined by transient absorption of the Si wafer, is typically <180 fs.

Theoretical studies on hydrogen-bonded imidazole···XO (X = N or C) complexes were performed using the GAUSSIAN 03 program.[23] The geometries of both complexes, XO···imidazole and OX···imidazole, were fully optimized using the DFT/B3LYP method with the 6-31g(d) basis as a function of hydrogen bond angle ∠HXO (angle H···XO) or ∠HOX (angle H···OX). The H-bonding energy of the species was calculated at the optimized geometry for the fixed hydrogen bond angle.

As will be seen in the Results section, a significant portion of the deligated NO is in the vibrationally excited $v = 1$ state, resulting in a vibrationally hot absorption band ($v = 1 \rightarrow v = 2$). The relative hot band population was obtained by accounting for the absorbances of both the fundamental and hot band. Using the harmonic oscillator (HO) approximation for the absorbance, the integrated absorbance for the transition from the first vibrationally excited state, A_e, and the ground state, A_g, can be expressed as $A_e = 2\varepsilon n_e$ and $A_g = \varepsilon(n_g - n_e)$.[24] Here, n_e and n_g are the populations of NO in the first vibrationally excited state and in the ground state, respectively, and ε is the integrated absorption cross section for the fundamental band. Since $(n_g + n_e) = (A_g + A_e)/\varepsilon$ in the HO approximation, the population of a given state, $(n_g + n_e)$, can be represented by $(A_g + A_e)$ of the corresponding state.

III. RESULTS

Figure 1 shows time-resolved vibrational spectra of the stretching mode of NO after photodeligation of HbNO in D_2O at 283 K with a 580 nm pulse. The positive-going features at 1858 cm^{-1} arise from NO that was photodeligated from the Fe atom of the heme and remains in or near the heme pocket (B state),[8,25] while the negative-going features (bleach) at 1617 cm^{-1} result from the loss of bound NO (denoted as A state).[7] Both features appear faster than the time resolution of the instrument and decay in tens of picoseconds, which is consistent with the ultrafast photodeligation and ps GR observed using optical spectroscopy.[9,26−28] The fact that the

dx.doi.org/10.1021/jp3026495 | J. Phys. Chem. B 2012, 116, 6346−6355

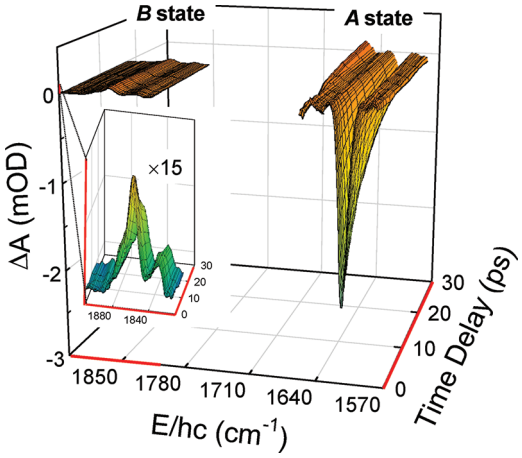

Figure 1. Time-resolved vibrational spectra of the stretching mode of NO after photolysis of HbNO in D_2O at 283 K. The positive-going signals arise from NO photodeligated from the heme and located near or in the heme pocket (B state), and the negative-going signals arise from the loss of bound NO (A state). Note that B-state spectra are about 30 times smaller than A-state ones, and 15-times-expanded B-state spectra are shown in the inset. The ordinate, $\Delta A(t)$, represents the pump-induced change in sample absorbance measured at pump−probe delay time t. The unit mOD represents 10^{-3} optical density (OD), i.e., 1 mOD = 10^{-3} OD. The raw data are shown even though A- and B-state spectra were collected with different sample path lengths and concentrations. Spectra of A state have to be scaled up ~5 times to normalize the sample condition.

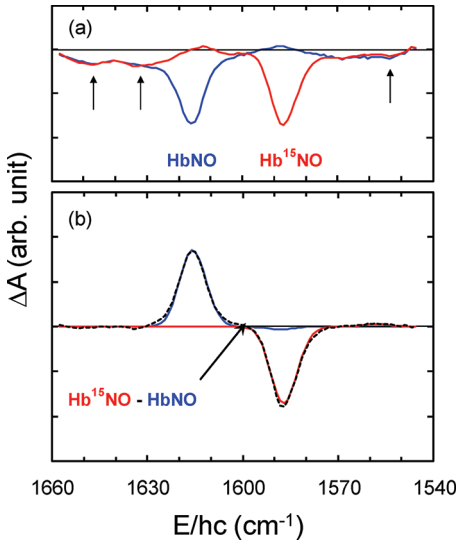

Figure 2. (a) Time-resolved A-state spectra of HbNO (blue line) and $Hb^{15}NO$ (red line) at a pump−probe delay of 0.6 ps. The spectral features consist of the NO band and a background signal arising from thermal and conformational relaxation of Hb after photodeligation. The background signal was modeled with the sum of a quadratic polynomial and Gaussian functions (see text). Arrows point to spectral features arising from conformational changes. (b) A difference spectrum ($Hb^{15}NO$ − HbNO, dashed line) is shown to reveal spectral features free from the signal arising from thermal and conformational changes. The background-free spectra (HbNO, blue line; $Hb^{15}NO$, red line) overlap the difference spectrum well, validating the background subtraction used here. Note that there is a small but apparent hot band in the background-free spectra.

absorbance is about 30 times smaller than the bleach is due to the dramatic reduction in the extinction coefficient of NO after it is deligated from the Fe atom.[8] The magnitude of the new absorption (bleach) corresponds to ~9% (22%) photodeligation of HbNO. A higher proportion of the sample is photolyzed in the A-state spectra because of the shorter path length of the sample.

Ligand-Bound States of HbNO. The spectral region of the bound NO is congested with the amide band of the protein as well as a small but broad absorption due to a combination of bending and libration modes of the D_2O solvent at 1555 cm^{-1} with a ~200 cm^{-1} full width at half-maximum (fwhm) (ε_{max} = 1.91 M^{-1} cm^{-1}).[29] These spectral features are sensitive to the protein conformation as well as the temperature of the protein and solvent. The NO band was assigned using a ^{15}NO-ligated sample ($Hb^{15}NO$). A quadratic polynomial was used to represent the featureless background arising from the heating of solvent, thermal cooling of photodeligated Hb and geminately recombined but partially relaxed HbNO, and cooling of the six-coordinate HbNO that relaxes without being photodeligated.[7,15] There were small features in the wings of the bound NO band (arrows in Figure 2a). They were also observed in the signals of the photolysis of MbNO and MbCO and have been attributed to the conformational relaxation of the photodeligated protein.[7,30] They were well described by Gaussian functions. The bound NO band was obtained by subtracting the quadratic background and Gaussians arising from conformational relaxation from the measured spectra. As shown in Figure 2b, the background-free spectra compare well with the difference spectrum between HbNO and $Hb^{15}NO$, which reveals a spectral feature directly related to the bound NO bands, validating the assignment of the bound NO band and the background subtraction used here. The bound NO band appears to be a single feature, but two Gaussians (denoted to A_{G1} and A_{G2}) resulted in much better fit (see Figure 3). The A_{G1} band on the higher energy side decays faster than the A_{G2} band on the lower energy side. Both bands contribute about the same magnitude to the bound NO band. Spectral evolution in the bleach band clearly demonstrates the NO band in HbNO consists of two bands and they decay with different time scale. The decay kinetics of each band was obtained (see Supporting Information). However, since two bands are merged into a single feature, the kinetic parameters of the bands could be very sensitive to the background subtraction. Thus, we did not pursue further interpretation of the kinetic parameters of two bands.

As shown in the next section, about 13% of the deligated NO is in the v = 1 state with a vibrational relaxation (VR) time of ~200 ps, and it rebinds on a ps time scale. Thus, as the NO rebinding progresses, since vibrationally excited NO also rebinds, the rebound NO has a vibrationally hot absorption band of NO in HbNO as well as its fundamental absorption band. The hot band decays with a VR time of the first vibrationally excited NO in HbNO, which is very different from that of the deligated NO, ~200 ps. The fundamental absorption band from the rebound NO reduces the magnitude of the initial bleach. Without the NO in the v = 1 state, the population of the deligated Hb is represented by the magnitude of the remaining bleach. With the NO in the v = 1 state, since the population of the NO in the v = 1 state, n_e contributes to both the fundamental band, $A_g = \varepsilon(n_g - n_e)$ and the hot band, $A_e = 2\varepsilon n_e$, the population of the deligated Hb was obtained by the magnitude of the remaining bleach minus the magnitude of the hot band in HbNO. Since the VR time and anharmonicity of the hot NO band in HbNO are not known, and the signal-to-

dx.doi.org/10.1021/jp3026495 | J. Phys. Chem. B 2012, 116, 6346−6355

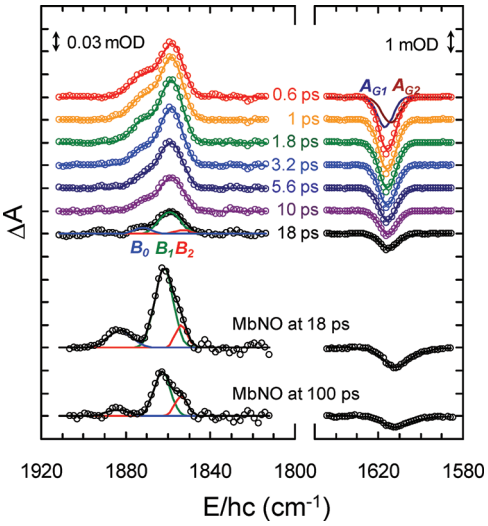

Figure 3. Representative time-resolved vibrational spectra of the stretching mode of NO after photolysis of HbNO. Data are offset to avoid overlap. For clarity, background signals due to thermal and conformational relaxation have been subtracted from the measured spectra. For simplicity, the vibrationally hot band has also been subtracted from the spectra (see text). Evolving spectra are well described by the sum of three (B state) or two (A state) Gaussians (○, data; —, fit). The B-state spectrum at 18 ps is decomposed into three Gaussians labeled B_0, B_1, and B_2. For comparison, time-resolved spectra of MbNO at 18 and 100 ps are shown on the bottom.[8] The A-state spectrum at 0.6 ps is also decomposed into two Gaussians labeled A_{G1} and A_{G2} (see text).

noise (S/N) ratio of our data is not good enough to extract this information, we measured the VR time and anharmonicity of the hot band of NO in a model heme, 1-methlyimidazole-hemin-NO. This resulted in a VR time of 3 ± 0.3 ps and an anharmonicity of 31 ± 2 cm^{-1}.[31] These parameters were used to fit the hot band of the bound NO in HbNO. Because of the fast VR time, the magnitude of the hot band was smaller than 6% of that of the bleach. The hot band contribution, although clearly visible, is small in the background-free spectra (see Figure 2b).

The recovery kinetics of the HbNO population after photodeligation was obtained from the time-dependent change of the bleach and the hot band of HbNO. The recovery kinetics was found to be nonexponential, suggesting that the GR of photodeligated NO to Hb is nonexponential at room temperature in aqueous solution, as was observed for Mb. The recovery kinetics can be described by a double-exponential function, 0.54 exp(−t/5.6 ps) + 0.46 exp(−t/29 ps). The fitted time constants are intended not to represent independent motion but to serve as parameters characterizing the nonexponentiality of the NO rebinding.[7] The nonexponential GR of NO to heme protein has also been described by a time-dependent rebinding rate.[6,7,9] The time-dependent rebinding rate $k_{gr}(t)$ was obtained by introducing a time-dependent barrier $E(t)$ into the Arrhenius equation, $k(t) = A \exp[-E(t)/RT]$, with $E(t) = (E_0 - E_{eq}) \exp(-k_{bar}t) + E_{eq}$, where k_{bar} is the rate constant for the variation in the barrier height from its initial height E_0 to its equilibrium value E_{eq}.[6,7,9] While fitting the data, we found that both heights for the varying barrier cannot be determined uniquely by the rebinding kinetics alone. In principle, there is no barrier initially, i.e., the initial height E_0 = 0 kcal/mol. A previous experiment on the rebinding of NO to Hb indicated that E_0 = 0.000 67 kcal/mol.[9] Either value resulted in similar values for the remaining rate parameters. Here, for the sake of the simplicity, we used the literature value, E_0 = 0.000 67 kcal/mol. The recovery kinetics of HbNO population was also fitted to the time-dependent rebinding rate, resulting in $A = 1.4 \times 10^{11}$ s^{-1}, k_{bar} = (44 ps)$^{-1}$, and E_{eq} = 1.6 kcal/mol. From these values, time constants in the limit are calculated to be 7 ps at t = 0 and 120 ps at $t = \infty$. These recovered parameters are comparable with those obtained from optical spectroscopy.[9]

Photoproduct States of HbNO. The spectral region of NO photodeligated from HbNO is free from any protein absorption but has a small background absorption due to the tail of the weak but ∼200 cm^{-1} wide band of D_2O at 1555 cm^{-1}.[29] The solvent band can shift and broaden as the temperature of the solvent increases. A featureless baseline shift, attributed to a change of the solvent absorbance due to thermal relaxation of the photoexcited protein, was modeled by a quadratic polynomial and subtracted for clarity. The remaining two distinctive features (see the inset of Figure 1) exhibit a ^{15}NO isotopic shift, suggesting that the bands arise from NO. The major feature near 1858 cm^{-1} consists of several bands, and the minor feature near 1830 cm^{-1} is a red-shifted replica of the major one. In the major feature, the shoulder on the high-energy side is described by a single band and denoted as B_0.[8,25] The middle peak at 1858 cm^{-1} appears to be a single feature, but it is described by two evolving bands (denoted B_1 and B_2). These assignments are based on a similar experiment on MbNO, where the bands are more separated and GR is slower. Thus, in MbNO, the bands are better distinguished and the spectral evolution is better observed. As can be seen in the bottom of Figure 3, while the B_1 and B_2 bands are clearly distinguished in the spectrum of NO photodeligated from MbNO at 100 ps, they are not apparent at 18 ps, as they are not in the features of HbNO. The peak on the higher energy side (B_0 band) is also more apparent in MbNO (see Figure 3). The feature near 1830 cm^{-1} is attributed to the v = 1 → v = 2 transition of NO (hot band) because it is a replica of the major feature on the high-energy side that is red-shifted by 28 cm^{-1}. This value is similar to the anharmonicity of NO in the gas phase, 27.94 cm^{-1}.[32] In view of the large v = 1 band, there might be another hot band near 1802 cm^{-1} that results from v = 2 to v = 3 transition. However, the limited S/N ratio in our data could not warrant any significant band at 1802 cm^{-1}. Thus, the band from the v = 2 state was not accounted for in our analysis.

As mentioned before, multiple vibrational bands for the ligand photodissociated from the Fe atom of the heme result from different positions and/or orientations of the ligand within or near the heme pocket in a given CS of the protein.[18] The existence of several CSs is manifested by a distribution of band positions, resulting in a Gaussian band shape. Three vibrational bands for the deligated NO from HbNO suggest that the deligated NO likely resides in three B sites, as does that from MbNO. To characterize the spectral evolution of the assigned bands, the raw spectra were fitted to a sum of three evolving Gaussians with their red-shifted replicas and quadratic polynomials. Initially, the spectral parameters of three bands were allowed to vary independently. Both the center frequency of B_1 and the fwhm of B_0 varied exponentially with time, but the changes in the remaining center frequencies and FWHMs were negligibly small. Thus, in the final global fitting of the whole B-state spectra, exponential time constants were used for

dx.doi.org/10.1021/jp3026495 | J. Phys. Chem. B 2012, 116, 6346−6355

the time evolutions of these two parameters, and the other center frequencies and FWHMs were kept constant. These constraints did not much affect the kinetics of the integrated absorbance of each band. The fitted parameters for the three Gaussians are plotted in Figure 4. The spectral evolution of the

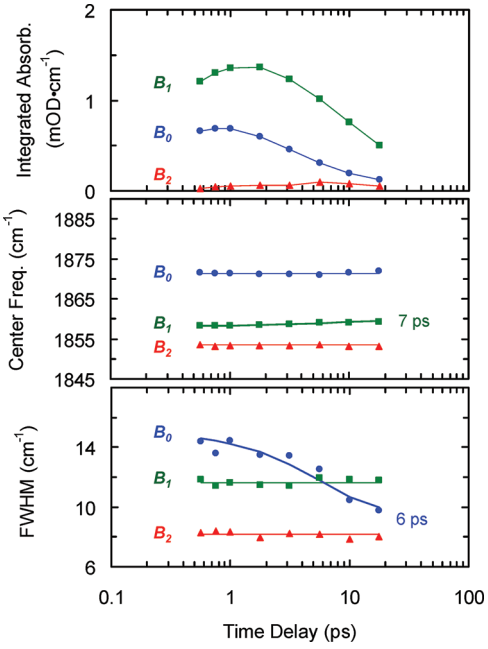

Figure 4. Fitted parameters of the B-state spectra for three Gaussians representing the three B states. The thick solid lines with time constants are exponential fits to the fitted parameters (symbols), and the thin solid lines are to guide the eyes.

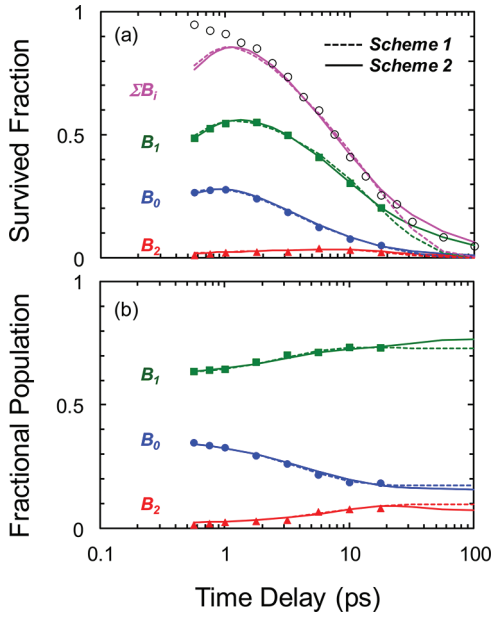

Figure 5. (a) Time-dependent change in the survived fractions of the three B states (filled symbols) and the deligated Hb population obtained from the A-state kinetics (open circles). (b) Time dependence of the fractional B-state population. The data are fitted to the two kinetics schemes described in the text (dashed lines, Scheme 1; solid lines, Scheme 2). The survived fraction represents the remaining deligated Hb when the initial population of the deligated Hb and the total integrated area of the B states are set to 1. The initial rise in the integrated areas of the B states was manifested by using the estimated total integrated area in the absence of structural reorganization during the initial rise. The fractional population was obtained by dividing each absorbance area by the total integrated area.

B state of HbNO is very similar to that of MbNO, except that the magnitude of the evolution in Hb is smaller than in Mb. The position of the B_1 band shifts slightly blueward with a time constant of 7 ps, and the bandwidth of B_0 narrows with a time constant of 6 ps. These time constants are similar to those of the B-state spectra in MbNO, HbCO, and MbCO. This spectral evolution likely arises from conformational relaxation of Hb after photolysis. Conformational relaxation on this time scale has also been observed in the amide band[30,33] and band III[34,35] of photolyzed MbCO. As shown in Figure 5a, the total integrated B-state absorbance exhibits an initial growth before it decays on the ps time scale. This initial growth, also observed in MbNO, HbCO, and MbCO, has been attributed to structural reorganization of the neighboring protein residues surrounding the nascent docked ligand after deligation.[8,30,36] In contrast to B_0 and B_1, B_2 has a much slower growth time than the other B states (see Figure 4), suggesting that factors other than the structural rearrangement contribute to the increase in B_2, such as NO population change due to transitions between B states (see below). The integrated area of each band is related to the NO population in each B site.[8] Thus, except for the initial fast growth, the change in the integrated area of each band directly accounts for the change in the population of NO in the site. The NO population in a B site can change as a result of ligand interconversion among B sites as well as GR to the heme. Interconversion among B states can be clearly manifested by a time-dependent fractional population that is obtained by dividing each B band by the total integrated area. The fractional population (Figure 5b) shows transitions among the three B states and that they tend to approach equilibrium with one another.

It is known that, at room temperature, the B bands are a portion of the whole spectrum of the photolyzed ligand. The integrated absorbance of the photodeligated ligand has been suggested to be partitioned between narrow B bands and a broad unresolved pedestal, the partitioning of which is determined by the orientational constraints imposed on the unbound ligand by the surrounding protein.[8,36−38] The more constrained the deligated ligand, the smaller the amplitude of its librational motion, and the greater the integrated absorbance under the narrow B-state features.[37] As mentioned, the initial growth of the integrated area has been attributed to protein rearrangement, which serves to constrain the orientation of the ligand in the heme pocket.[36] Recent time-resolved IR spectroscopy on CO photolyzed from MbCO and HbCO showed that the fractional population of photolyzed CO is well represented by the relative integrated absorbance of the B bands.[39] This suggests that the integrated absorbance of the B band, even though it may have a broad feature and the partitioning between the broad feature and the B band may be time dependent, is a good representation of the population of the photodeligated ligand in the designated site.

About 30% of the main band appears in the hot band of the deligated NO (see the inset of Figure 1), which is similar to (higher than) that observed in the photolysis of MbNO (HbCO and MbCO), where ca. 40% (10%) of the main band was observed in the hot band.[8,30,37,40] When ligated heme protein is photolyzed, more NO molecules than CO molecules

dx.doi.org/10.1021/jp3026495 | J. Phys. Chem. B 2012, 116, 6346−6355

dissociate with higher vibrational energy. Evidently, energy transfer from an impulsive half-collision into the ligand vibration is more efficient in the photolysis of NO-ligated heme protein than in that of the CO-ligated one.[41] Since NO binds in a bent configuration and CO in a linear configuration, the NO might be deligated with more rotational energy. Thus, when ligated heme protein is photolyzed, the departing NO may have more rotational energy as well as more vibrational energy than the CO, suggesting that the translational energy of the departing NO is likely smaller than that of the CO. As discussed before, since the population of a given B state ($n_g + n_e$) is represented by ($A_g + A_e$) of the corresponding B state in the HO approximation, the kinetics of the population change in a given B state is represented by the time-dependent sum of the integrated absorbances of the fundamental band (A_g) and the hot band (A_e) for the corresponding B state. When the whole spectra of the photodeligated NO were globally fitted, a nascent vibrationally excited NO population of 13 ± 3% (of the deligated NO) and an NO VR time of larger than ~100 ps were obtained from the kinetics of the relative amplitude of the red-shifted absorbance. Since the VR time could not be well-defined with the data spanning only up to 18 ps and the environments for the deligated NO in Hb is very similar to that in Mb, it was fixed at 200 ps in the final global fitting. This value, 200 ps, was obtained from the fitting of the B-state spectra of MbNO, where the data span up to 100 ps. However, 200 ps should be viewed as a rough estimate for the VR time of NO in the heme pocket because the recovered value is larger than the span of the data even in MbNO, and the S/N ratio of the data is limited. Fortunately, the other parameters recovered from the fit were negligibly influenced by the VR time of NO.

Modeling Kinetics of the B Bands. For B-state spectra arising from ligands photodeligated from MbNO, HbCO, and MbCO, the integrated absorbance of each B site has been suggested to be proportional to the population of the unbound ligand in the corresponding site.[8,30,36,37] We also assumed that the population of NO in each site is proportional to the integrated absorbance of the corresponding B band. Thus, the time dependence of the integrated absorbance contains information about the GR rate of the deligated NO, the transition rates among B states, and the VR of the excited NO. Including all these factors affecting the population of NO in the B states, we have tried various kinetics schemes to describe both the kinetic behaviors of three B bands and the recovery kinetics of the HbNO population. For all the kinetics schemes, the rates for the transitions and rebinding of NO are assumed to be independent of its vibrational energy, as found in a recent molecular dynamics (MD) simulation.[42] Here, the two most relevant kinetics schemes are described in detail.

Scheme 1 is the most general kinetics model with time-independent rates for GR and interconversion among B states. In Scheme 1, all three B states can directly rebind to heme and interconvert to one another with time-independent rates. Even though rebinding from all three B states is allowed, in the fitted results the rebinding from one state, B_0 was enough to reproduce the kinetic behaviors of all B states and the recovery kinetics of the HbNO population. Scheme 1 fit the kinetics of the B bands very well up to 18 ps and the recovery kinetics of the HbNO population very well up to 32 ps, and it results in almost complete GR by 80 ps. However, the GR of NO to Hb is highly nonexponential, and more than 5% of the deligated NO is still unbound at 100 ps.[28] A recent experiment on photolysis of MbNO, where GR is slower than in HbNO and thus the interconversion dynamics can be observed for a longer period, showed that a time-dependent rebinding rate is necessary to reproduce the integrated B-state absorbance change. The time-dependent rebinding rate was described by $k(t) = A \exp[-E(t)/RT]$, which was also used to fit the recovery kinetics of the HbNO population (see above).[8] Interconversion of NO among B states in Mb as well as that of CO among B states in Mb and Hb, where ligands interconvert without rebinding, are well described by time-independent rates.[39] Therefore, in addition to Scheme 1, which has only time-independent rates, we tested a kinetics scheme incorporating a time-dependent rebinding rate and time-independent interconversion rates. In Scheme 2, a time-dependent rate is incorporated in the GR from B_1. The rest of the rebinding rates and all the interconversion rates are set to be time independent. The kinetics schemes and their parameters recovered from the global fit of the whole spectra are shown in Figure 6. Since the data span less than 100 ps, rate constants much slower than $(100\ \text{ps})^{-1}$ are set to zero and deleted in the final fit. Interestingly, in both kinetics schemes, although all three B states are allowed to rebind, one rebinding channel was sufficient to reproduce the kinetics of all three B bands and the recovery kinetics of the HbNO population. Since the nascent population of B_2 is negligible, a kinetics scheme with time-dependent rebinding from B_2 is not discussed here.[8]

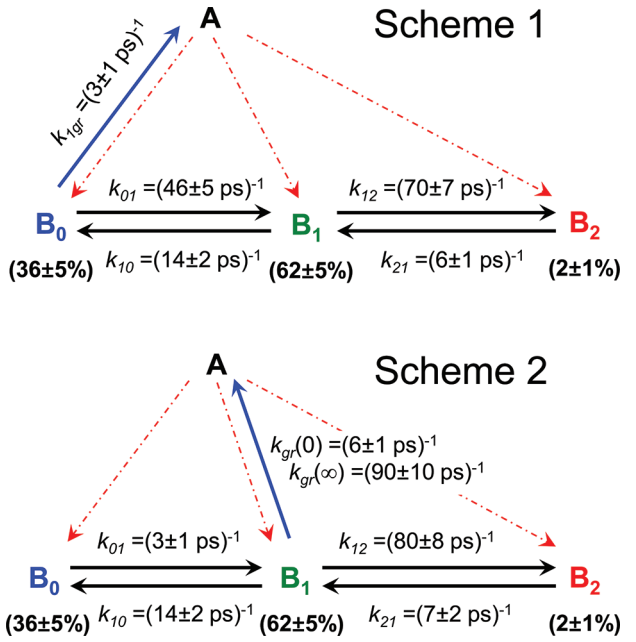

Figure 6. Two kinetics schemes used to fit the time evolution of the B-state spectra and the recovery kinetics of the HbNO population and their best-fit parameters. Red dot-dashed arrows represent pathways of the ligand photodeligated from the heme, and solid arrows represent interconversion among B states (black lines) as well as GR from them (blue lines). Whereas each scheme contains all the possible interconversions among the three B states and GR from them, transitions with rate constants much slower than $(100\ \text{ps})^{-1}$ are removed in the fitting. In the case of time-dependent GR from B_1 in Scheme 2, GR rates at delay times of $t = 0$, $k_{gr}(0)$, and $t = \infty$, $k_{gr}(\infty)$, are shown.

Up to 32 ps, the quality of the fit is excellent in the two kinetics schemes explored here (see Figure 5). However, Scheme 1 deviates from the recovery kinetics of the HbNO

dx.doi.org/10.1021/jp3026495 | J. Phys. Chem. B 2012, 116, 6346−6355

population at later times (see Figure 5a), and thus Scheme 2 is a more appropriate model for HbNO, as it was for MbNO. A few parameters are found to be independent of the kinetics scheme used. These include the rise time of the total integrated areas of the B states, the initial partitioning of NO, and the hot band population and VR time of NO. The recovered rise time of the integrated B-state absorbance was 0.4 ± 0.2 ps. This rise time is in reasonable agreement with those found in MbNO (0.6 ± 0.2 ps) and MbCO experiments (1.1 ± 0.1 ps),[36,39] suggesting that the growth results from protein reorganization, as suggested. Following the initial rise, the total integrated area of a B state reproduces the time dependence of the recovery of the HbNO population (Figure 5a),[7] confirming that the B states indeed arise from NO photolyzed from HbNO and its integrated area represents the population of the deligated NO in the corresponding site. The initial partitioning of the NO photolyzed from HbNO was 36 ± 5% in B_0, 62 ± 5% in B_1, and 2 ± 1% in B_2, which matches well that obtained from MbNO, where it was 41 ± 6% in B_0, 57 ± 5% in B_1, and 2 ± 1% in B_2.[8] As in the MbNO, photolysis leads from A to mainly B_0 and B_1, and B_1 thermally exchanges with B_0 and B_2. NO rebinds primarily from B_1, and the recovered rate constant for the time-dependent change in the barrier height is $(39 \pm 5\ \text{ps})^{-1}$, slower than that in Mb, $(15 \pm 2\ \text{ps})^{-1}$;[8] this is consistent with the suggestion that the change in the barrier height results from conformational relaxation of the protein. Although Scheme 2 is successful in describing state-specific kinetics of NO rebinding to Hb, it may not be a unique solution explaining kinetic behavior of NO rebinding to Hb. However, it can serve as a good working scheme that satisfies all the kinetic characteristics observed in the rebinding of the deligated NO and the population recovery of HbNO.

IV. DISCUSSION

HbNO is known to undergo ultrafast photodeligation upon Soret-band or Q-band excitation.[11] Since the bond energy of Fe-NO, ~88 kJ/mol,[43] is smaller than the photon energy of 116 kJ/mol (a 580 nm photon), excess energy is distributed into the heme, Fe atom, and departing NO. The detailed partitioning of this excess energy depends on features of the mechanism of photodeligation, such as the electronic states of Hb involved in the photodeligation of NO.[26] It was suggested that the CO photodeligated from HbCO can leave the heme with a supersonic velocity due to its initial kinetic energy, but it immediately encounters other atoms in the heme pocket, and its motion becomes diffusive.[41] Indeed, using a reactive MD simulation, Karplus and co-workers showed that the excess kinetic energy of the NO photodeligated from Mb is thermalized within 300 fs.[42] Since photodeligated NO assumes diffusive motion immediately after photolysis and there is no space in the heme pocket large enough for NO to move freely, it likely resides near the Fe atom in the time range of ps.

Using MD simulations of CO photolyzed from MbCO, Karplus and co-workers found that CO was constrained within an L-shaped thin slab containing two higher probability regions located 1.3 and 2.3 Å from the heme normal.[44] The equilibrium orientations of CO in these two regions were nicely correlated with the orientational distribution of CO calculated from polarization anisotropy spectra of the B state measured by time-resolved polarized mid-IR spectroscopy after photolysis of MbCO and HbCO.[20] On the basis of this correlation, Anfinrud and co-workers suggested that the B_1 and B_2 states of photolyzed CO spectra arise from CO in the regions 1.3 and 2.3 Å from the heme normal, respectively, and they are roto-isomers each other.[20] They also hypothesized that while B_1 and B_2 can interconvert freely under ambient conditions, ligand binding proceeds through B_1, the region nearer the heme Fe.[20] The locations of the L-shaped thin slab regions are consistent with the primary docking site for CO found in time-resolved[45−47] as well as cryogenic crystallography measurements.[48−51] Since a globular protein is in general highly packed, and a ligand can reside only in structured cavities, the photodeligated NO likely occupies the same or a similar location as CO in globular heme proteins. Since bound CO is normal to the heme plane but bound NO is severely bent,[52] the translational energy of NO departing after photoexcitation is likely smaller than that of CO. Therefore, most of the nascent photolyzed NO likely goes to the nearby bound site rather than the farther site. The smaller relative initial population in B_2 of NO than of CO can be attributed to the lower kinetic energy in the photodeligated NO by assigning B_2 to a farther location than B_1 or B_0.

The vibrational band for the ligand deligated from MbNO was blue-shifted from the gas-state value, and thus it was assigned to B_0.[8] By comparing the B-state spectra of HbNO and MbNO, a band in HbNO, even though it is not blue-shifted as much as that in MbNO, was also assigned to the B_0 band. The kinetic behaviors of the band intensity, position, and fwhm of the B_0 band of HbNO are very similar to those of MbNO,[8] corroborating the band assignment. However, the B_0 band was not observed in any of the data reported for MbNO photolysis at cryogenic temperatures.[53,54] To the best of our knowledge, no data on the transient IR absorption of NO in Hb have been reported. In experiments on MbCO photolysis at cryogenic temperature, a significant amount of B_0 was observed when a short illumination period of the photolysis light was used.[55] When extended illumination or a continuous tungsten light source was used for the photolysis, the B_0 band in MbCO showed strong sample-to-sample variation,[25,55] suggesting that B_0 is unstable and quickly rebinds or interconverts into other states. The absence of the B_0 band at cryogenic temperature in MbNO data[53,54] is likely due to the continuous photolysis source, which caused unstable B_0 to interconvert to more stable B_1. As mentioned before, the Fe−NO bond energy is smaller than the photon energy used for photolysis, and thus excess energy heats up the heme by a few hundreds of degrees,[56] even for the cryogenic-temperature samples. Since thermal relaxation of the heated heme takes a few ps,[56−58] the ligand deligated from protein at cryogenic temperature is sandwiched between a hot heme and cold protein during the thermal relaxation. The ligand is eventually quenched into a low-temperature distribution that is not in thermal equilibrium but is kinetically trapped. The lack of a B_0 band in MbNO data obtained at cryogenic temperatures was attributed to a rapid interconversion from unstable B_0 to B_1 during the thermal relaxation.[8] The fastest decay of the B_0 band in HbNO is consistent with the notion that unstable B_0 interconverts to B_1, quickly losing its nascent population after photolysis.

The blue-shift in the B_0 band was suggested to arise from an H bond between the distal histidine and the N atom of NO.[8] Interestingly, the B_0 band was observed after photolysis of HbNO and MbNO at room temperature but absent after photolysis of HbCO and MbCO at room temperature. The B_0 band in MbCO was also blue-shifted from the gas-state value[25] and was suggested to arise from an H bond between the distal histidine and the C atom of CO.[59] It appears that the B_0 band

dx.doi.org/10.1021/jp3026495 | J. Phys. Chem. B 2012, 116, 6346−6355

requires a cavity within the heme pocket facilitating an H bond between the distal histidine and the X atom of XO ligand. As shown in Figure 7, CO forms the most stable H bond with an

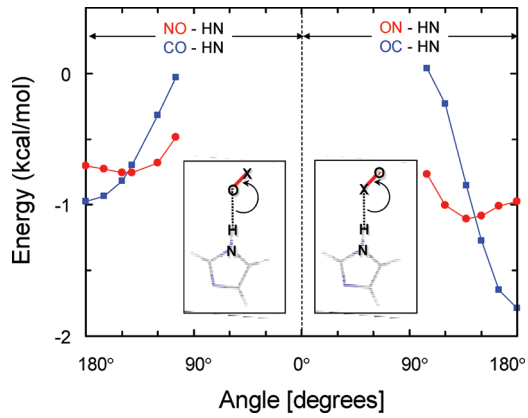

Figure 7. Calculated H-bonding energy versus the pointing angle of NO and CO to imidazole, the model for the distal histidine in the heme protein.

imidazole, the model for the distal histidine, in a linear geometry, i.e., $\angle(\mathrm{HCO}) = 180°$, but NO forms the most stable H bond when $\angle(\mathrm{HNO}) = \sim 138°$. If the geometry of the heme cavity that accommodates the deligated ligand allows only a severely bent configuration for H bonding with the distal histidine, i.e., $\angle(\mathrm{HXO}) < 138°$, the spectral feature for the deligated ligand in the cavity would show up only for NO, as observed for HbNO or MbNO. The rapid interconversion between B_0 and B_1 indicates that B_0 is located very close to B_1. The fast appearance of the B_0 band suggests that its location is as near as that of B_1. According to MD simulations performed by Meuwly and co-workers on NO deligated from MbNO at different temperatures, below 250 K the deligated NO solely goes to the "center of the distal pocket", a location adjacent to the Fe atom but different from the primary docking site found in various theoretical and experimental investigations after photolysis of MbCO. However, it goes both to the center of the distal pocket and to the primary docking site when MbNO is deligated at 300 K.[60] Although the temperature-dependent behavior in the simulation is not consistent with the observed B bands, considering that the center of the distal pocket is another site capable of accommodating a ligand and it is within H-bonding distance from the distal histidine, it is tempting to assign the B_0 band to the NO in the center of the distal pocket. Time-resolved crystallography with a ps time resolution would be useful for clearly identifying the location of the NO deligated from MbNO and HbNO.

The recovery kinetics of the HbNO population, as well as the decay of its B-state spectra, confirms that the kinetics for GR of the NO photodissociated from HbNO in room-temperature aqueous solution is nonexponential and occurs on the ps time scale, as found in previous optical transient absorption spectroscopy experiments.[9,26−28] GR of NO to the heme in MbNO also has nonexponential kinetics with a slower rate than that in HbNO. Clearly, nonexponential kinetics is a characteristic of GR of NO to Mb and Hb, even in room-temperature aqueous solution. The nonexponential rebinding of NO to Mb and Hb could arise from a distribution of rebinding barriers resulting from various protein conformations that interconvert slower than the rebinding, multiple sites for the deligated NO within the protein, and/or a time-dependent barrier resulting from protein relaxation on the time scale of the rebinding process.[7,8] Although the two CSs of MbNO showed the same rebinding kinetics, the two Gaussian bands in HbNO, even though they are not as distinctive as in MbNO, showed different rebinding kinetics. It is possible that these two bands, which have about equal intensity, arise from the α and β subunits of HbNO in the $\alpha_2\beta_2$ tetrameric structure. Interestingly, the $\sim$2.6 cm^{-1} separation between the two vibrational bands of HbNO is comparable to the 1.1 cm^{-1} separation between those that were assigned to the vibrational bands of α and β subunits of HbCO.[61] Therefore, the nonexponential rebinding of NO to Hb arises not only from the structural inhomogeneity of HbNO but also from the multiple sites for the deligated NO that have different rebinding kinetics and interconvert with each other. Furthermore, the time-dependent barrier resulting from conformational relaxation also contributes to the nonexponential rebinding of NO to Hb in aqueous solution at room temperature.

If the two bands in HbNO arise from α and β subunits of HbNO, each subunit may have different B state spectra and different NO rebinding kinetics. Incorporating the heterogeneity due to the α and β subunits into B state kinetics results in too many degrees freedom. Since the heme pocket of the α and β subunits, where the deligated NO resides in, is well preserved, B state spectra and the NO rebinding kinetics are likely similar in both subunits. Here, for the sake of simplicity, the subunit heterogeneity in B state spectra was accounted for by Gaussian line shape in the spectra and B state kinetics was assumed to be the same in both subunits. B-state spectra for an isolated subunit and its rebinding kinetics of NO would certainly be useful to test the present assumption.

The Fe atom is known to undergo out-of-plane motion upon photodeligation of HbNO, and thus it will move back to the heme plane upon NO rebinding. Whereas heme doming occurs quasi-instantaneously with NO deligation,[28] the heme dedoming in Hb is found to be delayed by a time constant of 15 ps after NO binding.[28] Clearly, NO binds to a domed heme and subsequently the NO-bound Fe moves back to the heme plane. The NO absorption band for the HbNO in a domed configuration may be different from that for equilibrium structure of HbNO. Therefore, the observed spectral evolution in the bleach in HbNO may arise from the different NO band in the domed heme configuration from equilibrium one. The spectral evolution of the bleach can arise from conformation-dependent rebinding as well as the delayed heme dedoming. When the observed spectral evolution of the bleach was treated assuming conformation-independent rebinding, the band shifted with $\sim$30 ps time constant, which is larger than reported 15 ps. Thus, it cannot be attributed to the delayed heme dedoming alone. Furthermore, since the spectral evolution is strongly influenced by the background subtraction, the present data do not warrant neither a reliable recovery of the NO absorption band in the domed configuration nor trustworthy conformation-dependent kinetic parameters. Here, for the sake of simplicity, we attributed the spectral evolution in the bleach of HbNO to the subunit-dependent NO rebinding and neglected the possible influence of the delayed heme dedoming on the spectral evolution. Although the spectral evolution in the bleach spectra can be interpreted differently, the main conclusion of the present work, the suggested rebinding pathway is not affected by the assignment of the spectral evolution of the bleach.

dx.doi.org/10.1021/jp3026495 | J. Phys. Chem. B 2012, 116, 6346−6355

V. CONCLUSION

Femtosecond mid-IR spectra of deligated NO after photolysis of HbNO in D_2O at room temperature show that the deligated NO occupies three sites (B_0, B_1, and B_2) within the heme pocket, translocates among these sites, and rebinds from them. Conformation-specific kinetics in HbNO and the direct observation of the deligated NO within Hb have revealed that the nonexponential rebinding of NO to Hb arises from structural inhomogeneity of HbNO, multiple sites for the deligated NO, and the time-dependent rebinding barrier arising from conformational relaxation. The three B sites were assigned by comparing the B-band characteristics with those observed in MbCO and MD simulations: B_0 is the center of the distal pocket that was observed in an MD simulation,[60] and B_1 and B_2 are the two sites closer to and farther from the Fe atom in the primary docking site, respectively, where deligated CO is located after photolysis of MbCO and HbCO. A kinetics scheme incorporating rebinding from the B_1 site with a time-dependent rebinding barrier and time-independent interconversion among the three sites most successfully describes the kinetic behaviors of the three B bands and the recovery kinetics of the HbNO population. We envisioned the NO motion after photodeligation of HbNO as follows. The photodeligated NO primarily goes to the center of the distal pocket and the location closer to the Fe atom in the primary docking site. Both sites are nearer to the Fe atom than the third site. A small fraction of the deligated NO goes to the third site, the location farther from the Fe atom in the primary docking site, too. The NO in the center of the distal pocket is unstable and rapidly equilibrates with the closer primary docking site, which also equilibrates with the farther primary docking site, and the rebinding occurs via the closer primary docking site, the rebinding barrier of which increases as the protein conformation relaxes toward the deligated structure. The NO motion after deligation from Hb is very similar to that from Mb, suggesting that the heme pocket near the Fe atom is well preserved in both HbNO and MbNO.

■ ASSOCIATED CONTENT

Supporting Information

Figure S1. This material is available free of charge via the Internet at http://pubs.acs.org.

■ AUTHOR INFORMATION

Corresponding Author

*E-mail: mhlim@pusan.ac.kr.

Notes

The authors declare no competing financial interest.

■ ACKNOWLEDGMENTS

This work was supported by the National Research Foundation of Korea (NRF) grant funded by the Korea government (MEST) (No. 2011-0016114).

■ REFERENCES

(1) Springer, B. A.; Sligar, S. G.; Olson, J. S.; Phillips, G. N., Jr. *Chem. Rev.* **1994**, *94*, 699−714.

(2) Austin, R. H.; Beeson, K. W.; Eisenstein, L.; Frauenfelder, H.; Gunsalus, I. C. *Biochemistry* **1975**, *14*, 5355−5373.

(3) Henry, E. R.; Sommer, J. H.; Hofrichter, J.; Eaton, W. A. *J. Mol. Biol.* **1983**, *166*, 443−451.

(4) Gibson, Q. H.; Regan, R.; Elber, R.; Olson, J. S.; Carver, T. E. *J. Biol. Chem.* **1992**, *267*, 22022−22034.

(5) Walda, K. N.; Liu, X. Y.; Sharma, V. S.; Magde, D. *Biochemistry* **1994**, *33*, 2198−2209.

(6) Petrich, J. W.; Lambry, J. C.; Balasubramanian, S.; Lambright, D. G.; Boxer, S. G.; Martin, J. L. *J. Mol. Biol.* **1994**, *238*, 437−444.

(7) Kim, S.; Jin, G.; Lim, M. *J. Phys. Chem. B* **2004**, *108*, 20366−20375.

(8) Kim, S.; Lim, M. *J. Am. Chem. Soc.* **2005**, *127*, 8908−8909.

(9) Petrich, J. W.; Lambry, J. C.; Kuczera, K.; Karplus, M.; Poyart, C.; Martin, J. L. *Biochemistry* **1991**, *30*, 3975−3987.

(10) Shreve, A. P.; Franzen, S.; Simpson, M. C.; Dyer, R. B. *J. Phys. Chem. B* **1999**, *103*, 7969−7975.

(11) Petrich, J. W.; Poyart, C.; Martin, J. L. *Biochemistry* **1988**, *27*, 4049−4060.

(12) Ikeda-Saito, M.; Dou, Y.; Yonetani, T.; Olson, J. S.; Li, T.; Regan, R.; Gibson, Q. H. *J. Biol. Chem.* **1993**, *268*, 6855−6857.

(13) Quillin, M. L.; Li, T.; Olson, J. S.; Phillips, G. N., Jr.; Dou, Y.; Ikeda-Saito, M.; Regan, R.; Carlson, M.; Gibson, Q. H.; et al. *J. Mol. Biol.* **1995**, *245*, 416−436.

(14) Kholodenko, Y.; Gooding, E. A.; Dou, Y.; Ikeda-Saito, M.; Hochstrasser, R. M. *Biochemistry* **1999**, *38*, 5918−5924.

(15) Ye, X.; Demidov, A.; Champion, P. M. *J. Am. Chem. Soc.* **2002**, *124*, 5914−5924.

(16) Carver, T. E.; Rohlfs, R. J.; Olson, J. S.; Gibson, Q. H.; Blackmore, R. S.; Springer, B. A.; Sligar, S. G. *J. Biol. Chem.* **1990**, *265*, 20007−20020.

(17) Carlson, M. L.; Regan, R.; Elber, R.; Li, H.; Phillips, G. N., Jr.; Olson, J. S.; Gibson, Q. H. *Biochemistry* **1994**, *33*, 10597−10606.

(18) Mourant, J. R.; Braunstein, D. P.; Chu, K.; Frauenfelder, H.; Nienhaus, G. U.; Ormos, P.; Young, R. D. *Biophys. J.* **1993**, *65*, 1496−1507.

(19) Ansari, A.; Berendzen, J.; Braunstein, D. K.; Cowen, B. R.; Frauenfelder, H.; Hong, M. K.; Iben, I. E. T.; Johnson, J. B.; Ormos, P.; et al. *Biophys. Chem.* **1987**, *26*, 337−355.

(20) Lim, M.; Jackson, T. A.; Anfinrud, P. A. *J. Am. Chem. Soc.* **2004**, *126*, 7946−7957.

(21) Moller, J. K. S.; Skibsted, L. H. *Chem. Rev.* **2002**, *102*, 1167−1178.

(22) Bredenbeck, J.; Hamm, P. *Rev. Sci. Instrum.* **2003**, *74*, 3188−3189.

(23) Gaussian 03: Frisch, M. J.; Trucks, G. W.; Schlegel, H. B.; Scuseria, G. E.; Robb, M. A.; Cheeseman, J. R.; Montgomery, J. A.; , Jr., Vreven, T.; Kudin, K. N.; Burant, J. C. et al. Gaussian, Inc., Wallingford, CT, 2004.

(24) Wilson, E. B.; Decius, J. C.; Cross, P. C. *Molecular Vibrations: The Theory of Infrared and Raman Vibrational Spectra*; Dover: New York, 1955.

(25) Alben, J. O.; Beece, D.; Bowne, S. F.; Doster, W.; Eisenstein, L.; Frauenfelder, H.; Good, D.; McDonald, J. D.; Marden, M. C.; et al. *Proc. Natl. Acad. Sci. U. S. A.* **1982**, *79*, 3744−3748.

(26) Cornelius, P. A.; Hochstrasser, R. M.; Steele, A. W. *J. Mol. Biol.* **1983**, *163*, 119−128.

(27) Rohlfs, R. J.; Olson, J. S.; Gibson, Q. H. *J. Biol. Chem.* **1988**, *263*, 1803−1813.

(28) Kruglik, S. G.; Yoo, B.-K.; Franzen, S.; Vos, M. H.; Martin, J.-L.; Negrerie, M. *Proc. Natl. Acad. Sci. U. S. A.* **2010**, *107*, 13678−13683.

(29) Venyaminov, S. Y.; Prendergast, F. G. *Anal. Biochem.* **1997**, *248*, 234−245.

(30) Kim, S.; Heo, J.; Lim, M. *Bull. Korean Chem. Soc.* **2005**, *26*, 151−156.

(31) Park, J.; Lee, T.; Lim, M. Manuscript in preparation, 2012.

(32) Herzberg, G. *Spectra of Diatomic Molecules*; Van Nostrand Reinhold Ltd.: New York, 1950.

(33) Causgrove, T. P.; Dyer, R. B. *J. Phys. Chem.* **1996**, *100*, 3273−3277.

(34) Kuczera, K.; Lambry, J. C.; Martin, J. L.; Karplus, M. *Proc. Natl. Acad. Sci. U. S. A.* **1993**, *90*, 5805−5807.

(35) Lim, M.; Jackson, T. A.; Anfinrud, P. A. *Proc. Natl. Acad. Sci. U. S. A.* **1993**, *90*, 5801−5804.
(36) Lim, M.; Jackson, T. A.; Anfinrud, P. A. *Nat. Struct. Biol.* **1997**, *4*, 209−214.
(37) Lim, M.; Jackson, T. A.; Anfinrud, P. A. *J. Chem. Phys.* **1995**, *102*, 4355−4366.
(38) Kriegl, J. M.; Nienhaus, K.; Deng, P.; Fuchs, J.; Nienhaus, G. U. *Proc. Natl. Acad. Sci. U. S. A.* **2003**, *100*, 7069−7074.
(39) Kim, S.; Lim, M. *J. Am. Chem. Soc.* **2005**, *127*, 5786−5787.
(40) Kim, S.; Lim, M. *Bull. Korean Chem. Soc.* **2006**, *27*, 1825−1831.
(41) Anfinrud, P. A.; Han, C.; Hochstrasser, R. M. *Proc. Natl. Acad. Sci. U. S. A.* **1989**, *86*, 8387−8391.
(42) Meuwly, M.; Becker, O. M.; Stote, R.; Karplus, M. *Biophys. Chem.* **2002**, *98*, 183−207.
(43) Nutt, D. R.; Meuwly, M. *Biophys. J.* **2006**, *90*, 1191−1201.
(44) Vitkup, D.; Petsko, G. A.; Karplus, M. *Nat. Struct. Biol.* **1997**, *4*, 202−208.
(45) Schotte, F.; Lim, M.; Jackson, T. A.; Smirnov, A. V.; Soman, J.; Olson, J. S.; Phillips, G. N., Jr.; Wulff, M.; Anfinrud, P. A. *Science* **2003**, *300*, 1944−1947.
(46) Schotte, F.; Soman, J.; Olson, J. S.; Wulff, M.; Anfinrud, P. A. *J. Struct. Biol.* **2004**, *147*, 235−246.
(47) Hummer, G.; Schotte, F.; Anfinrud, P. A. *Proc. Natl. Acad. Sci. U. S. A.* **2004**, *101*, 15330−15334.
(48) Schlichting, I.; Berendzen, J.; Phillips, G. N., Jr.; Sweet, R. M. *Nature* **1994**, *371*, 808−812.
(49) Teng, T. Y.; Srajer, V.; Moffat, K. *Nat. Struct. Biol.* **1994**, *1*, 701−705.
(50) Hartmann, H.; Zinser, S.; Komninos, P.; Schneider, R. T.; Nienhaus, G. U.; Parak, F. *Proc. Natl. Acad. Sci. U. S. A.* **1996**, *93*, 7013−7016.
(51) Teng, T.-Y.; Srajer, V.; Moffat, K. *Biochemistry* **1997**, *36*, 12087−12100.
(52) Brucker, E. A.; Olson, J. S.; Ikeda-Saito, M.; Phillips, G. N., Jr. *Proteins: Struct., Funct., Genet.* **1998**, *30*, 352−356.
(53) Miller, L. M.; Pedraza, A. J.; Chance, M. R. *Biochemistry* **1997**, *36*, 12199−12207.
(54) Nienhaus, K.; Palladino, P.; Nienhaus, G. U. *Biochemistry* **2008**, *47*, 935−948.
(55) Abadan, Y.; Chien, E. Y. T.; Chu, K.; Eng, C. D.; Nienhaus, G. U.; Sligar, S. G. *Biophys. J.* **1995**, *68*, 2497−2504.
(56) Henry, E. R.; Eaton, W. A.; Hochstrasser, R. M. *Proc. Natl. Acad. Sci. U. S. A.* **1986**, *83*, 8982−8986.
(57) Lingle, R., Jr.; Xu, X.; Zhu, H.; Yu, S. C.; Hopkins, J. B. *J. Phys. Chem.* **1991**, *95*, 9320−9331.
(58) Lim, M.; Jackson, T. A.; Anfinrud, P. A. *J. Phys. Chem.* **1996**, *100*, 12043−12051.
(59) Straub, J. E.; Karplus, M. *Chem. Phys.* **1991**, *158*, 221−248.
(60) Nutt, D. R.; Meuwly, M. *ChemPhysChem* **2004**, *5*, 1710−1718.
(61) Potter, W. T.; Hazzard, J. H.; Kawanishi, S.; Caughey, W. S. *Biochem. Biophys. Res. Commun.* **1983**, *116*, 719−725.